Design and Performance Analysis of a New M-ary Differential Chaos Shift Keying with Index Modulation

Xiangming Cai, Weikai Xu, *Member, IEEE,* Meiyuan Miao, Lin Wang, *Senior Member, IEEE*

***Abstract*—A new M-ary differential chaos shift keying with index modulation (IM-MDCSK), which has the advantages of high data rate and low energy consumption, is proposed in this paper. In the proposed scheme, each data frame is divided into several time slots where the reference signal is placed in the first time slot and the rest time slots with specific indices are provided for information bearing signals. More exactly, the information bearing signals with active indices are modulated by M-ary DCSK symbols, and the active indices are determined by mapped bits via the combination number mapping method. At the receiver, the absolute values of decision variables in all branches are used to find the indices of active time slots, while M-ary DCSK demodulation is applied to recover the modulated bits. Moreover, we derive the analytical bit-error-rate (BER) expressions for the proposed scheme over additive white Gaussian noise (AWGN) and multipath Rayleigh fading channels, and then simulation results verify our theoretical derivations. Finally, the performance of IM-MDCSK scheme is compared with M-ary DCSK and other up-to-date chaotic modulation schemes based on index modulation (IM). IM-MDCSK scheme is proved to be competitive and preeminent.**

***Index Terms*—High data rate, enhanced M-ary DCSK, index modulation, bit-error-rate (BER).**

I. Introduction

Chaotic signals are derived from the nonlinear dynamical systems whose variables move in a bounded, non-periodic, random-like fashion. Indeed, there are impulse-like auto-correlation and low cross-correlation values for chaotic signals, which are attributed to their noise-like property. Being broadband, chaotic signals have been proven to be one of the excellent candidates for spread-spectrum (SS) communication systems and they intrinsically own the superiority of low probability of detection, anti-eavesdropping, anti-jamming and mitigation of multipath interference [1]–[3]. As a result, the above excellent features have attracted many researchers to conduct in-depth researches on chaotic signals and chaos-based communication schemes.

Actually, chaos-based communication schemes can be classified into two main categories, i.e., coherent scheme and non-coherent scheme. As a representative of coherent chaotic communication schemes, chaos shift keying (CSK) was first proposed in [4], where the locally-generated chaotic carriers have to be synchronized at receiver (i.e., chaos synchronization). Although many chaos-synchronization algorithms have been proposed in [5], [6], unfortunately, perfect chaos synchronization is still a challenging task today, which restricts the development and application of coherent scheme. In contrast, without the demand of complicated chaos synchronization and channel estimation, non-coherent schemes have attracted a lot of interests. As a type of non-coherent schemes, differential chaos shift keying (DCSK) [7] and its frequency-modulated version (FM-DCSK) [8] show strong robustness against multipath degradation. Therefore, DCSK scheme has been applied in many different communication scenarios, such as simultaneous wireless information and power transfer system [9], continuous mobility communication system [10] and power line communication system [11].

In conventional DCSK scheme, each data frame is uniformly divided into two time slots for the transmission of reference signal and information bearing signal, respectively. In detail, the reference chaotic signal is sent in the first slot, while the information bearing signal is either identical or opposite to reference signal and transmitted in the second slot. As a transmitted-reference (TR) system, however, DCSK inherently suffers from two main drawbacks. Firstly, half of the symbol duration is spent to transmit non-information-bearing reference samples [1], which results in low data rate and much energy waste. Secondly, the usage of long wide-band delay line creates obstacles to implement in CMOS technology [12]. [1]

Apparently, the tremendous demands of high data rate and energy efficiency are, and will continue to be key elements for wireless communication systems. Accordingly, many non-coherent chaotic communication schemes have been proposed to improve the data rate and energy efficiency. Considering M-ary modulation schemes, an M-ary version of DCSK called quadrature chaos shift keying (QCSK) [14] can gain double data rate with the same bandwidth occupation and similar bit error rate performance of DCSK. Based on QCSK scheme, a circle-constellation-based M-ary DCSK was proposed in [15], which offers better BER performance than M-ary PSK-DCSK system (MPSK-DCSK) [16]. In addition, a multi-resolution M-ary DCSK (MR-M-DCSK) was presented in [15], which increases the data rate and provides different quality of service (QoS) for various transmitted bits within a symbol. Motivated by the above researches, a square-constellation-based M-

Xiangming Cai, Weikai Xu, Meiyuan Miao and Lin Wang are with the Department of Information and Communication Engineering, Xiamen University, Xiamen, P. R. China. (e-mail: samson0102@qq.com, xweikai@xmu.edu.cn, meiyuanmiao@foxmail.com, wanglin@xmu.edu.cn). This work was supported by the National Natural Science Foundation of China under Grant No. 61671395 and 61871337.

[1]Note that the wideband Radio Frequency (RF) delay lines is an issue under the analog modulation scenario, but it is not a matter anymore when the digital system design becomes more credible [13].

ary DCSK was proposed in [17], which can obtain higher energy efficiency with lower complexity, but it suffers from high peak-to-average power ratio (PAPR). In particular, a new hierarchical square-constellation-based M-DCSK scheme [18], which is also applicable to other constellations, such as rectangular, star and asymmetrical square constellations, can provide lower energy consumption and achieve excellent BER performance in contrast to MR-M-DCSK scheme.

Different from the conventional multilevel modulation scheme [19], generalized code-shifted DCSK (GCS-DCSK) [20] and multilevel CS-DCSK (MCS-DCSK) [21] have the advantages of lower complexity and higher spectral efficiency. A high-data-rate CS-DCSK scheme (HCS-DCSK) was presented in [22] where different chaotic codes are chosen to separate reference and information signals, instead of the limited Walsh codes. The orthogonal multilevel DCSK (OM-DCSK) was presented in [23], where its information bearing signals are derived from the orthogonal signal set established by the original reference signal. Hence, OM-DCSK scheme can achieve higher data rate and energy efficiency, which are attributed to the abundant orthogonal signals.

A multi-carrier DCSK scheme (MC-DCSK) was introduced in [24], where the reference signal is sent over a predefined subcarrier and the multiple modulated data streams are sent over the remaining orthogonal subcarriers. Based on this work, the optimal power allocation strategy [25] and noise-reduction method [26] were applied to MC-DCSK system to improve its BER performance in [27], [28]. A multiuser multi-carrier DCSK (MU-OFDM-DCSK) was proposed in [29], which is a combination of OFDM and DCSK. MU-OFDM-DCSK scheme supports multiple access (MA) communication and improves the energy efficiency with low complexity.

In the past few years, index modulation (IM) has developed rapidly, where the activated index as an information bearing unit increases the data rate and spectral efficiency [30]. As a new IM technique, code index modulation (CIM) was first proposed by Kaddoum *et al.* and CIM was applied to direct-sequence spread-spectrum (DSSS) where the indices of spreading codes are used to convey extra information in addition to the transmitted symbols [31], [32]. There are two types of multilevel chaotic modulation schemes with CIM, called CIM-CS-DCSK [33] and CIM-MCS-DCSK [34] respectively, which can carry additional mapped bits by specific code indices. By constructing a signal set where all of the constructed signals are orthogonal to reference signal, permutation index DCSK (PI-DCSK) [13] and commutation code index DCSK (CCI-DCSK) [35] were proposed to increase the data rate. Furthermore, by exploiting the permutation set, an efficient multiple access method was applied in PI-DCSK system. More recently, a novel short reference DCSK (SR-DCSK) [36] with code index modulation and its optimization versions which greatly improve its BER performance were presented in [37]. With regard to carrier index modulation schemes, carrier index DCSK (CI-DCSK) [38] and its M-ary version (CI-MDCSK) [39] were proposed to improve energy and spectral efficiency.

Additionally, SR-DCSK scheme [36] makes reference signal shorter than information bearing signal to reduce frame duration, leading to data rate increase and bit energy saving. Enhanced DCSK scheme was proposed in [40] where the reference signal is followed by more than one information bearing signal which improves the data rate and reduces energy waste. By recycling each reference sample in DCSK scheme, high-efficiency DCSK scheme (HE-DCSK) [41] can transmit two bits within a symbol duration, which offers higher data rate compared to DCSK scheme. In order to reduce the number of delay lines in HE-DCSK scheme, a reference-modulated DCSK scheme (RM-DCSK) was proposed in [42] where its reference signal also serves as information bearing unit which increases its data rate.

In this paper, we propose a new M-ary DCSK scheme with index modulation, namely IM-MDCSK scheme. To better illustrate the proposed scheme, we firstly extend enhanced DCSK scheme [40] into its M-ary version, namely enhanced M-ary DCSK. Then, the above enhanced M-ary DCSK and index modulation make a powerful combination to further increase the data rate and spectral efficiency. The main contributions of this paper are summarized as follows:

- A new M-ary differential chaos shift keying scheme with index modulation is proposed, where index modulation technique is used to select the transmission time slots of information bearing signals.
- After analyzing and comparing the spectral efficiency and hardware complexity of IM-MDCSK and other chaotic modulation systems, we find that the hardware complexity of IM-MDCSK system is generally higher than CIM-DCSK, PI-DCSK and CCI-DCSK systems. Whereas, the spectral efficiency of IM-MDCSK system with reasonable parameters is superior to its rivals.
- The theoretical BER expressions of IM-MDCSK system are derived over AWGN and multipath Rayleigh fading channels, and then simulation results validate our theoretical derivations. Additionally, in contrast to M-ary DCSK and other state-of-the-art IM-based non-coherent chaotic communication systems, IM-MDCSK system achieves excellent BER performance.

The remainder of this paper is organized as follows. The enhanced M-ary DCSK and its BER performance are given in Section II. The IM-MDCSK system model is presented in Section III. Besides, the spectral efficiency and hardware complexity of IM-MDCSK system are also analyzed in the same section. In Section IV, the BER performance analysis of IM-MDCSK system is given. The numerical results and discussions are presented in Section V. Section VI concludes this paper.

II. Enhanced M-ary DCSK System

A. System Model

In enhanced M-ary DCSK scheme, the reference and information bearing signals are transmitted in $1+N$ equal time slots. To be specific, the reference signal is placed in the first time slot and the rest time slots are occupied by N different information bearing signals. The block diagram of enhanced M-ary DCSK system is illustrated in Fig. 1. Firstly, at the transmitter, a reference chaotic signal with θ samples is generated from chaotic generator. Meanwhile, the

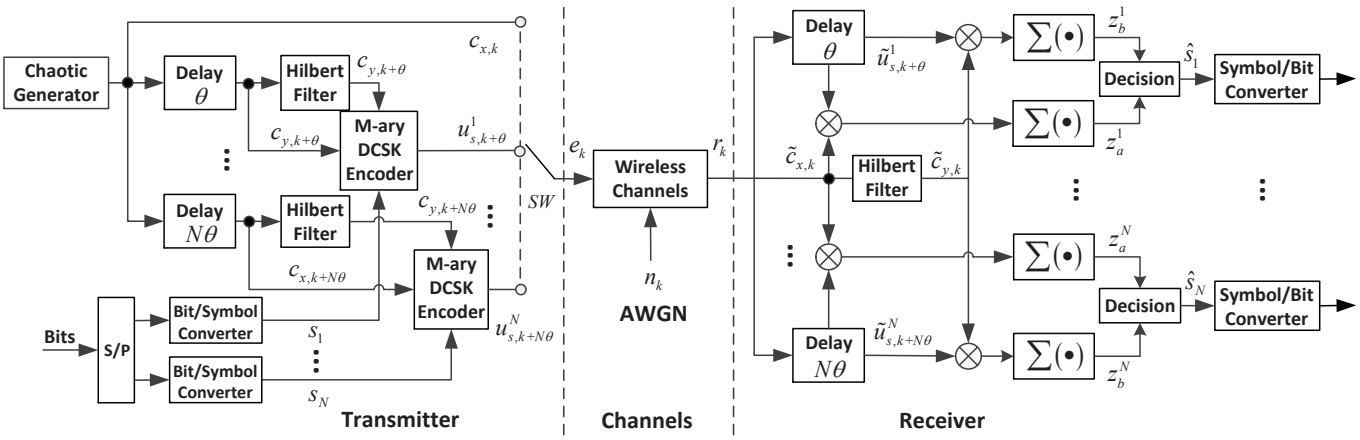

Fig. 1. The block diagram of enhanced M-ary DCSK system.

n^{th} delayed version of reference chaotic signal $c_{x,k+n\theta}$ is loaded into the n^{th} Hilbert filter and its orthogonal chaotic signal $c_{y,k+n\theta}$ is constructed. Then, the symbol information $s_n = a_n + \sqrt{-1}b_n$ on M-ary constellation point is encoded as a linear combination of the above orthogonal signals by M-ary DCSK encoder. Accordingly, the n^{th} information bearing signal is expressed as $u^n_{s,k+n\theta} = a_n c_{x,k+n\theta} + b_n c_{y,k+n\theta}$. Therefore, the transmitted signal of enhanced M-ary DCSK is given as

$$e_k = \begin{cases} c_{x,k}, \\ u^n_{s,k+n\theta}, \end{cases} \quad 1 \le k \le \theta, 1 \le n \le N, \tag{1}$$

where $c_{x,k}$ is a chaotic sequence with length θ generated by the logistic map $c_{x,j+1} = 1 - 2c^2_{x,j}, j \in Z^+$. Unlike M-ary DCSK scheme, clearly, the total number of transmitted bits within an enhanced M-ary DCSK symbol is equal to $n_t N$, where $n_t = \log_2 M$ is the number of transmitted bits in an M-ary constellation symbol and an enhanced M-ary DCSK symbol has N information bearing signals in total, where M denotes modulation order. Besides, we define a symbol period as spreading factor, namely $\beta = (1+N)\theta$.

At receiver, without loss of generality, considering the n^{th} information symbol, the received information bearing signal is correlated with reference signal and its orthogonal version which is transformed by Hilbert filter, thus the decision variables of in-phase branch z^n_a and quadrature branch z^n_b are obtained. Finally, the minimum distance decision criterion is applied to get the estimated n^{th} information symbol $\hat{s}_n$ as

$$\hat{s}_n = \arg\min_{s \in S} \left(\left| [z^n_a + \sqrt{-1} z^n_b] - s \right|^2 \right), \tag{2}$$

where S is M-ary constellation points set. Consequently, the original transmitted bits can be recovered by converting $\hat{s}_n$ from constellation symbols to bits.

B. Results

Particularly, the BER performance comparison between M-ary DCSK and MPSK-DCSK [16] has been carried out in [15], and it demonstrated that the performance of M-ary DCSK outperforms MPSK-DCSK slightly. Therefore, we choose M-ary DCSK as the contrast object for enhanced M-ary DCSK.

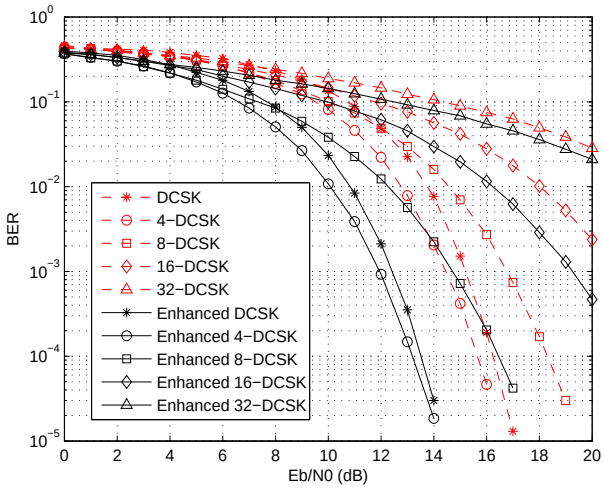

Fig. 2. Comparisons of BER performance between enhanced M-ary DCSK and M-ary DCSK over AWGN channel with $\beta = 128$, $N = 3$ and $M = 2, 4, 8, 16, 32$.

Fig. 2 compares the BER performance of enhanced M-ary DCSK and M-ary DCSK over AWGN channel. Clearly, enhanced M-ary DCSK scheme achieves large performance gain in comparison with M-ary DCSK scheme. For example, it offers enhanced M-ary DCSK about 3dB gain over M-ary DCSK at BER level 10^{-5} when modulation order is small (i.e., $M = 2$ or 4). Besides, the BER performance of both schemes are deteriorating when M increases. The main reason is that the decision boundaries of M-ary constellation decreases when M increases.

III. IM-MDCSK System

A. The Transmitter

Inspired by the high-performance enhanced M-ary DCSK scheme and applying index modulation to its time slots of information bearing signals, we propose a novel enhanced M-ary DCSK with index modulation, namely IM-MDCSK. The block diagram of IM-MDCSK transmitter is shown in Fig. 3. The total information bits are divided into several

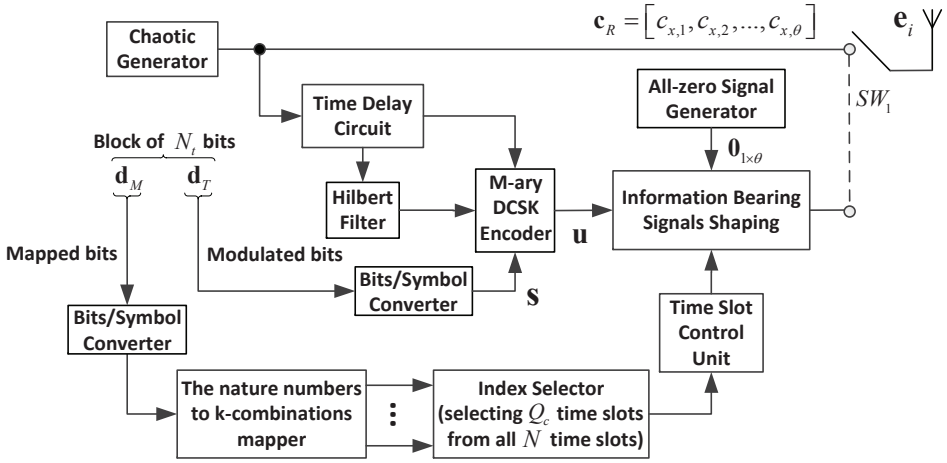

Fig. 3. The block diagram of IM-MDCSK transmitter.

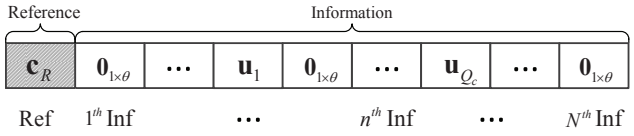

Fig. 4. One example for IM-MDCSK signal format.

blocks with N_t bits per block. The first sub-block with length m_c bits is provided for mapped bits, while the second sub-block with length $n_t Q_c$ bits is arranged for modulated bits. Therefore, the total number of the transmitted bits per block is $N_t = m_c + n_t Q_c$ and its vector form is presented as $\mathbf{d} = [d_1, d_2, \cdots, d_{m_c+n_t Q_c}] = [\mathbf{d}_M, \mathbf{d}_T]$ where $\mathbf{d}_M$ and $\mathbf{d}_T$ denote the vector of mapped bits and modulated bits, respectively.

The natural numbers to k-combinations mapping method [33], [43], where there is a one-to-one mapping between natural numbers and k-combinations, is adopted for converting mapped bits to the indices of the positions of selected time slots which are provided for information bearing signals. Moreover, as observed in Fig. 3, the time delay circuit outputs Q_c different delayed versions of reference signal, then the delayed reference signals and their orthogonal signals converted by Hilbert filter are loaded into M-ary DCSK encoder. Thus, Q_c disparate information bearing signals are constructed by different M-ary information symbols. Finally, the above Q_c information bearing signals and $N - Q_c$ all-zero signals generated by all-zero signal generator are sent into information bearing signals shaping circuit, hence the mixed information bearing signals come into being with the help of specific time slot index which comes from the time slot control unit.

One example for the frame format of IM-MDCSK signal is depicted in Fig. 4. According to the mapping method above, we choose Q_c time slots from all N time slots to transmit various information bearing signals where the indices of the selected time slots are converted from mapped bits and the rest $N - Q_c$ time slots are arranged for all-zero signals, i.e., no data bits are transmitted in those $N - Q_c$ time slots. Thus, the total number of mapped bits can be calculated as $m_c = \lfloor \log_2 \binom{N}{Q_c} \rfloor$, where $\binom{N}{Q_c} = \frac{N!}{Q_c!(N-Q_c)!}$ is combination number and $\lfloor \cdot \rfloor$ denotes floor function (e.g., $\lfloor 2.4 \rfloor = 2$). Generally, according to the above IM-MDCSK signal format, the transmitted baseband discrete signal of the i^{th} IM-MDCSK symbol is expressed as

$$\mathbf{e}_i = \left[\underbrace{\mathbf{c}_R}_{\text{reference}}, \underbrace{\mathbf{0}_{1\times\theta}, \cdots, \mathbf{u}_1, \mathbf{0}_{1\times\theta}, \cdots, \mathbf{u}_{Q_c}, \cdots, \mathbf{0}_{1\times\theta}}_{\text{information}} \right], \tag{3}$$

where $\mathbf{u}_1 = \left[u^1_{s,\theta+1}, u^1_{s,\theta+2}, \cdots, u^1_{s,2\theta} \right]$ denotes the vector of the first information bearing signal where $u^1_{s,\theta+1}$ is a linear combination of reference signal and its orthogonal version, i.e., $u^1_{s,\theta+1} = a_1 c_{x,\theta+1} + b_1 c_{y,\theta+1}$, $\mathbf{c}_R = [c_{x,1}, c_{x,2}, \cdots, c_{x,\theta}]$ is a discrete chaotic sequence with length θ. Other information bearing signals can be obtained in a similar manner. $\mathbf{0}_{1\times\theta} = [0, 0, \cdots, 0]$ is zero vector with a row and θ columns. The spreading factor of IM-MDCSK system is the same as enhanced M-ary DCSK system.

B. The Receiver

A classical channel model [24], [44] in wireless communication is considered in this paper. Assume that the transmitted signal is contaminated by multipath fading and additive white Gaussian noise, the received baseband discrete signal is written in a vector form as

$$\mathbf{r}_i = \sum_{l=1}^{L} \lambda_{i,l} \mathbf{e}_{i,\tau_{i,l}} + \mathbf{n}_i, \tag{4}$$

where L is the number of path, $\lambda_{i,l}$ and $\tau_{i,l}$ are the channel propagation coefficient and the appropriate time delay of the l^{th} path, respectively. And $\mathbf{n}_i$ denotes additive white Gaussian noise vector with zero mean and covariance $\frac{N_0}{2}\mathbf{I}$ where $\mathbf{I}$ is a unit matrix. Particularly, the channel degrades into AWGN channel when the channel parameters satisfy $L = 1$, a unit channel coefficient $\lambda_{i,1} = 1$ and zero time delay $\tau_{i,1} = 0$.

At IM-MDCSK receiver, the received baseband discrete signal is expressed in a vector form with one row and $(1 + N)\,\theta$ columns given as $\mathbf{r}_i = \left[r_1, r_2, \cdots, r_{(1+N)\theta} \right]$. In addition,

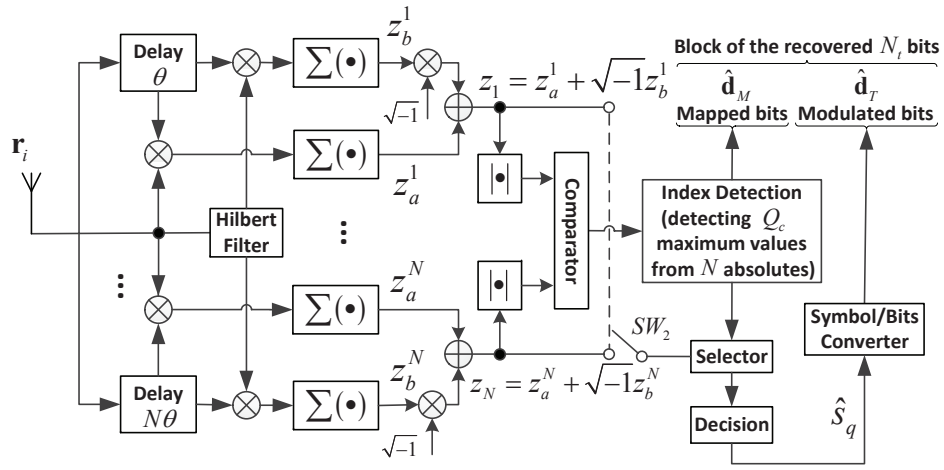

Fig. 5. The block diagram of IM-MDCSK receiver.

the subscript i will be omitted in the following analysis for simplicity. Accurately speaking, the front part of $\mathbf{r}_i$ is the received reference signal with length θ described as

$$\mathbf{r}_{\mathrm{ref}} = [r_1, r_2, \cdots, r_\theta]. \tag{5}$$

Similarly, other parts represent the n^{th} information bearing signal expressed as

$$\mathbf{r}_{\mathrm{inf},n} = \left[r_{n\theta+1}, r_{n\theta+2}, \cdots, r_{(n+1)\theta}\right], \quad n = 1, 2, \cdots, N. \tag{6}$$

As shown in Fig. 5, the reference signal and its orthogonal version are correlated with all possible information bearing signals, and the decision variables of the n^{th} in-phase and quadrature branches are described as

$$z_a^n = [\mathbf{r}_{\mathrm{ref}}]\left[\mathbf{r}_{\mathrm{inf},n}\right]^{\mathrm{T}}, \tag{7}$$

$$z_b^n = [\mathcal{H}(\mathbf{r}_{\mathrm{ref}})]\left[\mathbf{r}_{\mathrm{inf,n}}\right]^{\mathrm{T}}, \tag{8}$$

where $\mathcal{H}(\cdot)$ denotes Hilbert transform and $[\cdot]^{\mathrm{T}}$ represents transposition operation. Then, the linear combination of decision variable $z_n = z_a^n + \sqrt{-1}z_b^n$ is obtained. Let $|\mathbf{z}| = \{|z_1|, |z_2|, \cdots, |z_N|\}$, thus we can get Q_c indices which are according to Q_c maximums in set $|\mathbf{z}|$ by the demapping algorithm [33]. Then, let $|\mathbf{z}'| = \left\{|z_1'|, |z_2'|, \cdots, \left|z_{Q_c}'\right|\right\}$ be the selected Q_c maximums. Thus, the M-ary constellation symbols corresponding to the above Q_c maximums can be estimated by

$$\hat{s}_q = \arg\min_{s\in S}\left(|z_q' - s|^2\right), \ q = 1, 2, \cdots, Q_c. \tag{9}$$

Finally, the mapped bits are recovered by the estimated Q_c indices and the symbol-to-bits converter is used to recover the modulated bits.

C. Spectral Efficiency and Complexity Comparisons

In this subsection, the spectral efficiency and hardware complexity comparisons between IM-MDCSK system and other chaotic modulation systems are provided. Assuming the bandwidth is equal to B in all systems, we define the ratio of bit rate to total bandwidth as spectral efficiency [45]. According to the above subsections, there are $m_c + n_t Q_c$ bits transmitted in an IM-MDCSK symbol. As a result, the spectral efficiency of IM-MDCSK system is equal to $\frac{m_c+n_tQ_c}{(1+N)\theta B}$. The spectral efficiency comparison between IM-MDCSK system and other IM-based chaotic modulation systems is illustrated in Table I. Although the number of all permuted reference sequences in PI-DCSK scheme is numerous, which increases the number of mapped bits, this improvement is at the expense of complexity. Because permutation operation seems difficult for hardware implementation. Since index modulation and M-ary modulation are used in IM-MDCSK system, the total number of transmitted bits per symbol is large. Therefore, the spectral efficiency of IM-MDCSK system with reasonable parameters is superior to its rivals.

Table II and Table III show the transmitter and receiver complexities of IM-MDCSK, CIM-DCSK, PI-DCSK, and CCI-DCSK systems, respectively. Since many other blocks, such as time slot control unit, k-combinations mapper, all-zero signal generator, Hilbert filter and signal shaping, are required in IM-MDCSK system, the implementation of IM-MDCSK system is more complicated in contrast to its competitors. Moreover, Hilbert filter is used in both IM-MDCSK transmitter and receiver to realize M-ary modulation. Time delay circuit and delay line are also applied in IM-MDCSK system. In summary, the hardware complexity of IM-MDCSK system is generally higher than CIM-DCSK, PI-DCSK and CCI-DCSK systems.

TABLE I
SPECTRAL EFFICIENCY COMPARISON

Modulation Scheme	Spectral Efficiency
IM-MDCSK	$\frac{m_c+n_tQ_c}{(1+N)\theta B}$
CIM-DCSK	$\frac{m_c+1}{(1+2^{m_c})\theta B}$
PI-DCSK	$\frac{m_c+1}{2\theta B}$
CCI-DCSK	$\frac{m_c+1}{\theta B}$

TABLE II
TRANSMITTER COMPLEXITY COMPARISON

System	IM-MDCSK	CIM-DCSK	PI-DCSK	CCI-DCSK
Adders	0	0	0	1
Multipliers	0	2	1	2
Delay unit	Time delay circuit	Delay line	0	0
Selector	Index selector	Walsh code selector	Permutation selector	Index selector
Modulator	M-ary DCSK modulator	DCSK modulator	DCSK modulator	DCSK modulator
Other blocks	Time slot control unit, k-combinations mapper, all-zero signal generator, Hilbert filter, signal shaping	Walsh code generator	Permutation block	Commutation block, pulse shaping filter

TABLE III
RECEIVER COMPLEXITY COMPARISON

System	IM-MDCSK	CIM-DCSK	PI-DCSK	CCI-DCSK
Adders	$3N$	2^{m_c+1}	2^{m_c}	2^{m_c}
Multipliers	$3N$	2^{m_c}	2^{m_c}	$2^{m_c}+1$
Detection	Index detector	Code index detection	Index detector	Index detector
Demodulator	M-ary DCSK demodulator	DCSK demodulator	DCSK demodulator	DCSK demodulator
Other blocks	Hilbert filter, delay line	Walsh code generator, delay line	Permutation block, control unit	Commutation block, matched filter

IV. PERFORMANCE ANALYSIS

A. BER Analysis for IM-MDCSK System

According to the above analysis, there are $m_c + n_t Q_c$ transmitted bits in an IM-MDCSK symbol, where m_c bits are arranged for mapped bits and the rest $n_t Q_c$ bits are assigned for modulated bits. Therefore, the total BER of IM-MDCSK system is obtained by

$$P_{sys} = \frac{m_c}{m_c + n_t Q_c} P_{im} + \frac{n_t Q_c}{m_c + n_t Q_c} P_{em}, \tag{10}$$

where P_{im} and P_{em} represent the bit error probability of mapped bits and modulated bits, respectively. P_{im} is a function of erroneous index detection probability P_d, meanwhile P_{em} is a function of P_d and P_e, where P_e is the BER of modulated bits under the condition of correct index detection. When the index detection is incorrect, the number of wrong mapped bits per mapped symbol can take any values from 1 to m_c. The probability for detecting the incorrect mapped symbol is the same, which is equal to $\frac{1}{2^{m_c}-1}$. Thus the expectation of the number of wrong mapped bits per mapped symbol is calculated as

$$D = \sum_{i=1}^{m_c} i \frac{\binom{m_c}{i}}{2^{m_c}-1}. \tag{11}$$

Finally, the bit error probability of mapped bits is written as

$$P_{im} = \frac{D}{m_c} P_d. \tag{12}$$

As for the BER of modulated bits, there are two different cases that may lead to the wrong modulated bits. On one hand, the index detection is correct, but the modulated bits are demodulated incorrectly. On the other hand, there is an error in index detection. Consequently, the BER for modulated bits is given by

$$P_{em} = P_e (1 - P_d) + \frac{1}{2} P_d, \tag{13}$$

where the factor $\frac{1}{2}$ is the error probability of modulated bits when index detection is wrong, which means that the modulated bits based on incorrect index detection still have 50% chance of being correct. At last, substituting (12) and (13) into (10), the total BER of IM-MDCSK system can be rewritten as

$$P_{sys} = \frac{1}{m_c + n_t Q_c} \left[n_t Q_c (1 - P_d) P_e + \left(D + \frac{1}{2} n_t Q_c \right) P_d \right]. \tag{14}$$

B. Bit Error Probability P_e

Obviously, all the selected time slots of Q_c information bearing signals in an IM-MDCSK symbol are independent and have the same error probability, thus we merely need to evaluate the performance of one of them. Furthermore, the received signal in vector form may be a little tedious for our analysis, so the following analysis is performed with simple form of the received signal. Considering the output signal of the n^{th} correlator, we can get the n^{th} decision variable for in-phase branch in (15), as shown at the bottom of next page. Therefore, the mean and variance of decision variable z_a^n are calculated as

$$\mathrm{E}[z_a^n] = a_n \theta \sum_{l=1}^{L} \lambda_l^2 \mathrm{E}\left[c_k^2\right] = \sum_{l=1}^{L} \lambda_l^2 \frac{a_n E_s}{1 + Q_c}, \tag{16}$$

$$\begin{aligned} \mathrm{Var}[z_a^n] =& \theta N_0 \sum_{l=1}^{L} \lambda_l^2 \mathrm{E}\left[c_k^2\right] + \theta \frac{N_0^2}{4} \\ =& \sum_{l=1}^{L} \lambda_l^2 \frac{E_s N_0}{1 + Q_c} + \theta \frac{N_0^2}{4}, \end{aligned} \tag{17}$$

where $\mathrm{E}\left[c_k^2\right] = \mathrm{E}\left[c_{x,k+n\theta+\tau_l}^2\right] = \mathrm{E}\left[c_{x,k+\tau_l} c_{x,k+n\theta+\tau_l}\right] = \mathrm{E}\left[c_{y,k+n\theta+\tau_l}^2\right] = \mathrm{E}\left[c_{x,k+\tau_l}^2\right]$. Moreover, E_s denotes the symbol energy. Since only Q_c out of the N time slots are used to transmit various information bearing signals within an IM-MDCSK symbol and other time slots are zeros, the total symbol energy for an IM-MDCSK symbol satisfies

$E_s = \theta\left(1+Q_c\right)\mathrm{E}\left[c_k^2\right]$. Therefore, the relationship between the symbol energy and bit energy of IM-MDCSK system is given as

$$E_b = \frac{\theta\left(1+Q_c\right)\mathrm{E}\left[c_k^2\right]}{m_c + n_t Q_c} = \frac{E_s}{m_c + n_t Q_c}. \tag{18}$$

Similarly, the mean and variance of z_b^n are obtained as

$$\mathrm{E}[z_b^n] = \sum_{l=1}^{L} \lambda_l^2 \frac{b_n E_s}{1+Q_c}, \tag{19}$$

$$\mathrm{Var}[z_b^n] = \sum_{l=1}^{L} \lambda_l^2 \frac{E_s N_0}{1+Q_c} + \theta\frac{N_0^2}{4}. \tag{20}$$

According to the above analysis, the decision variables z_a^n and z_b^n can be regarded as independent Gaussian variables with means $m_1 = a_n E_m$ and $m_2 = b_n E_m$, respectively, where $E_m = \sum\limits_{l=1}^{L} \lambda_l^2 \frac{E_s}{1+Q_c}$. And both decision variables have the same variance $\sigma^2 = \sum\limits_{l=1}^{L} \lambda_l^2 \frac{E_s N_0}{1+Q_c} + \theta\frac{N_0^2}{4}$. When the symbol signal-to-noise ratio (SNR) is slightly large and $|\psi| \le \frac{\pi}{2}$, the bit error probability P_e is approximated as [46]

$$P_e \approx \frac{1}{n_t}\left[1 - \int_{-\frac{\pi}{M}}^{\frac{\pi}{M}} \frac{\mu\cos\psi}{\sqrt{2\pi}} \exp\left(-\frac{\mu^2 \sin^2\psi}{2}\right) \mathrm{d}\psi\right]. \tag{21}$$

where $\psi = \omega - \varphi$ denotes the phase error between the transmitted signal and the received signal which is contaminated by noise, as shown in Fig. 6. Moreover, $\mu = \frac{E_m}{\sigma}$ where $E_m = \sum\limits_{l=1}^{L} \lambda_l^2 \frac{E_s}{1+Q_c}$ and $\sigma^2 = \sum\limits_{l=1}^{L} \lambda_l^2 \frac{E_s N_0}{1+Q_c} + \theta\frac{N_0^2}{4}$. Accordingly, $\mu = \frac{2\gamma_s}{\sqrt{4(1+Q_c)\gamma_s + (1+Q_c)^2\theta}}$, where $\gamma_s = \sum\limits_{l=1}^{L} \lambda_l^2 \frac{E_s}{N_0}$ is the symbol SNR. Let $\nu = \mu\sin\psi$ and $\mathrm{d}\nu = \mu\cos\psi\mathrm{d}\psi$, P_e is further simplified as [47]

$$\begin{aligned} P_e \approx & \frac{2}{n_t\sqrt{2\pi}} \int_{\mu\sin\frac{\pi}{M}}^{+\infty} \exp\left(-\frac{\nu^2}{2}\right)\mathrm{d}\nu \\ = & \frac{2}{n_t} Q\left(\mu\sin\frac{\pi}{M}\right). \end{aligned} \tag{22}$$

where $Q(x) = \frac{1}{\sqrt{2\pi}}\int_x^{+\infty} \exp\left(-\frac{t^2}{2}\right)\mathrm{d}t$, $x \ge 0$.

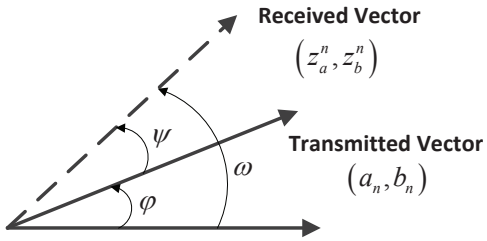

Fig. 6. Signal vector contaminated by noise.

C. Erroneous Index Detection Probability P_d

The detection method of the mapped indices is introduced in [33]. The mapped indices can be estimated by selecting a series of maximum absolute values of z_n where $z_n = z_a^n + \sqrt{-1}z_b^n$ is the linear combination of in-phase and quadrature branches corresponding to the n^{th} engaged correlator. When the largest absolute value of the n^{th} decision variable is less than the smallest absolute value of the m^{th} (desired) decision variable z_m for any $m \ne n$, the index detection is correct at this moment. Otherwise, there is an error. As a consequence, the erroneous index detection probability P_d can be expressed as

$$P_d = 1 - \Pr\left\{\max_{\substack{n\in\{1,2,\cdots,N-Q_c\}\\ n\ne m}} \{|z_n|\} < \min_{m\in\{1,2,\cdots,Q_c\}} \{|z_m|\}\right\}. \tag{23}$$

Obviously, since all correlators are irrelevant to each other, the above different random variables are independent. According to the above analysis, when index detection is correct, the mean and variance of z_m are given by

$$\begin{aligned} \mu_1 = & \mathrm{E}[z_a^m] + \mathrm{E}[z_b^m] = \sum_{l=1}^{L} \lambda_l^2 \frac{\left(a_m + b_m\right)E_s}{1+Q_c} \\ = & \sqrt{\sum_{l=1}^{L} \lambda_l^2 E_s N_0}\ \underbrace{\left(\frac{\left(a_m+b_m\right)\sqrt{\gamma_s}}{1+Q_c}\right)}_{\kappa}, \end{aligned} \tag{24}$$

$$\begin{aligned} z_a^n = & \sum_{k=1}^{\theta}\left[\sum_{l=1}^{L}\lambda_l c_{x,k+\tau_l} + n_k\right]\left[\sum_{l=1}^{L}\lambda_l\left(a_n c_{x,k+n\theta+\tau_l} + b_n c_{y,k+n\theta+\tau_l}\right) + n_{k+n\theta}\right] \\ = & \sum_{k=1}^{\theta}\sum_{l=1}^{L}\lambda_l^2 a_n c_{x,k+\tau_l} c_{x,k+n\theta+\tau_l} + \underbrace{\sum_{k=1}^{\theta}\sum_{l=1}^{L}\lambda_l^2 b_n c_{x,k+\tau_l} c_{y,k+n\theta+\tau_l}}_{=0} + \sum_{k=1}^{\theta}\sum_{l=1}^{L}\lambda_l c_{x,k+\tau_l} n_{k+n\theta} \\ & + \sum_{k=1}^{\theta}\sum_{l=1}^{L}\lambda_l\left(a_n c_{x,k+n\theta+\tau_l} + b_n c_{y,k+n\theta+\tau_l}\right) n_k + \sum_{k=1}^{\theta} n_k n_{k+n\theta} \end{aligned} \tag{15}$$

$$\begin{aligned}\sigma_1^2 =&\mathrm{Var}[z_a^m]+\mathrm{Var}[z_b^m]\\ =&2\left(\sum_{l=1}^{L}\lambda_l^2\frac{E_sN_0}{1+Q_c}+\theta\frac{N_0^2}{4}\right)\\ =&\sum_{l=1}^{L}\lambda_l^2E_sN_0\underbrace{\left(\frac{2}{1+Q_c}+\frac{\theta}{2\gamma_s}\right)}_{\alpha},\end{aligned}\tag{25}$$

where a_m and b_m are the real and imaginary parts of s_m. In particular, considering the situation of $M=2$, a_m and b_m are calculated as $a_m=\cos(0)$ or $a_m=\cos(\pi)$ and $b_m=\sin(0)$ or $a_m=\sin(\pi)$, respectively, namely $a_m=1$ and $b_m=0$. Thus, it is important to note that when $M=2$, the quadrature component z_b^m disappears, only leaving the in-phase component z_a^m. In this case, the mean and variance of z_m are obtained as $\mu_1=\kappa\sqrt{\sum_{l=1}^{L}\lambda_l^2E_sN_0}$ with $\kappa=\frac{\sqrt{\gamma_s}}{1+Q_c}$ and $\sigma_1^2=\alpha\sum_{l=1}^{L}\lambda_l^2E_sN_0$ with $\alpha=\frac{1}{1+Q_c}+\frac{\theta}{4\gamma_s}$.

Only Q_c out of N time slots are used for information bearing signals, and all-zero signals are transmitted in the remaining $N-Q_c$ time slots. At IM-MDCSK receiver, if an error occurs in index detection, the detected information bearing signals are all-zero signals contaminated by additive white Gaussian noises. In this case, the decision variable z_a^n is obtained as

$$\begin{aligned}z_a^n=&\sum_{k=1}^{\theta}\left(\sum_{l=1}^{L}\lambda_lc_{x,k+\tau_l}+n_k\right)n_{k+n\theta}\\ =&\sum_{k=1}^{\theta}\sum_{l=1}^{L}\lambda_lc_{x,k+\tau_l}n_{k+n\theta}+\sum_{k=1}^{\theta}n_kn_{k+n\theta}.\end{aligned}\tag{26}$$

Similarly, the decision variable z_b^n is stated as

$$z_b^n=\sum_{k=1}^{\theta}\sum_{l=1}^{L}\lambda_lc_{y,k+\tau_l}n_{k+n\theta}+\sum_{k=1}^{\theta}n_kn_{k+n\theta}.\tag{27}$$

Therefore, the mean and variance of z_n are calculated as

$$\mu_2=\mathrm{E}[z_a^n]+\mathrm{E}[z_b^n]=0,\tag{28}$$

$$\begin{aligned}\sigma_2^2=&\mathrm{Var}[z_a^n]+\mathrm{Var}[z_b^n]\\ =&2\left(\theta\sum_{l=1}^{L}\lambda_l^2\mathrm{E}\left[c_{x,k+\tau_l}^2\right]\frac{N_0}{2}+\theta\frac{N_0^2}{4}\right)\\ =&\sum_{l=1}^{L}\lambda_l^2\frac{E_sN_0}{1+Q_c}+\theta\frac{N_0^2}{2}\\ =&\sum_{l=1}^{L}\lambda_l^2E_sN_0\underbrace{\left(\frac{1}{1+Q_c}+\frac{\theta}{2\gamma_s}\right)}_{\Omega},\end{aligned}\tag{29}$$

Similar to the case of z_m, When $M=2$, the mean and variance of z_n are calculated as $\mu_2=0$ and $\sigma_2^2=\Omega\sum_{l=1}^{L}\lambda_l^2E_sN_0$ with $\Omega=\frac{1}{2(1+Q_c)}+\frac{\theta}{4\gamma_s}$, respectively.

The random variable z_m follows normal distribution $N\left(\mu_1,\sigma_1^2\right)$ with the mean $\mu_1=\kappa\sqrt{\sum_{l=1}^{L}\lambda_l^2E_sN_0}$ and variance $\sigma_1^2=\alpha\sum_{l=1}^{L}\lambda_l^2E_sN_0$, thus the random variable $|z_m|$ has a folded normal distribution. Besides, given a normally distributed random variable $z_n\sim N\left(\mu_2,\sigma_2^2\right)$, where $\mu_2=0$ and $\sigma_2^2=\Omega\sum_{l=1}^{L}\lambda_l^2E_sN_0$, the random variable $|z_n|$ meets a half-normal distribution. Hence, the probability density function of $|z_m|$, the cumulative distribution function of $|z_m|$ and $|z_n|$ are given as

$$f_{|z_m|}(x)=\frac{1}{\sqrt{2\pi\sigma_1^2}}\left\{e^{-\frac{(x-\mu_1)^2}{2\sigma_1^2}}+e^{-\frac{(x+\mu_1)^2}{2\sigma_1^2}}\right\},\tag{30}$$

$$F_{|z_m|}(x)=\frac{1}{2}\left[\mathrm{erf}\left(\frac{x-\mu_1}{\sqrt{2\sigma_1^2}}\right)+\mathrm{erf}\left(\frac{x+\mu_1}{\sqrt{2\sigma_1^2}}\right)\right],\tag{31}$$

$$F_{|z_n|}(x)=\mathrm{erf}\left(\frac{x}{\sqrt{2\sigma_2^2}}\right),\tag{32}$$

where $\mathrm{erf}(x)=\frac{2}{\sqrt{\pi}}\int_0^x e^{-t^2}\mathrm{d}t$, $x\geq 0$ denotes the well-known error function. To simplify the analysis, we define $Y=\min\{|z_m|\},m\in\{1,2,\cdots,Q_c\}$ and $X=\max(|z_n|),n\in\{1,2,\cdots,N-Q_c\}$, then the erroneous index detection probability P_d is derived as

$$\begin{aligned}P_d=&\int_0^{\infty}[1-\Pr\{X\leq y\}]f_Y(y)\,\mathrm{d}y\\ =&\int_0^{\infty}\left[1-\prod_{n=1}^{N-Q_c}\Pr\{|z_n|\leq y\}\right]f_Y(y)\,\mathrm{d}y,\end{aligned}\tag{33}$$

where $f_Y(y)$ is the probability density function of Y. Since Q_c random variables from $\{|z_1|,|z_2|,\cdots,|z_{Q_c}|\}$ are independent of each other, the cumulative distribution function of Y is stated as

$$F_Y(y)=1-\left[1-F_{|z_m|}(y)\right]^{Q_c}.\tag{34}$$

Then the probability density function of Y is the derivative of $F_Y(y)$, namely

$$f_Y(y)=Q_c\left[1-F_{|z_m|}(y)\right]^{Q_c-1}f_{|z_m|}(y).\tag{35}$$

Therefore the erroneous index detection probability in (33) can be further derived as

$$\begin{aligned}P_d=&\frac{1}{\sqrt{2\pi\sigma_1^2}}\int_0^{\infty}\left\{1-\left[\mathrm{erf}\left(\frac{y}{\sqrt{2\sigma_2^2}}\right)\right]^{N-Q_c}\right\}\\ &\times Q_c\left[1-F_{|z_m|}(y)\right]^{Q_c-1}\left\{e^{-\frac{(y-\mu_1)^2}{2\sigma_1^2}}+e^{-\frac{(y+\mu_1)^2}{2\sigma_1^2}}\right\}\mathrm{d}y.\end{aligned}\tag{36}$$

Let $y=\xi\sqrt{\sum_{l=1}^{L}\lambda_l^2E_sN_0}$ and $\mathrm{d}y=\sqrt{\sum_{l=1}^{L}\lambda_l^2E_sN_0}\mathrm{d}\xi$, we can

rewrite the above expression as

$$P_d = \frac{1}{\sqrt{2\pi\alpha}} \int_0^{\infty} \left\{ 1 - \left[\mathrm{erf}\left(\frac{\xi}{\sqrt{2\Omega}} \right) \right]^{N-Q_c} \right\} \times Q_c \left[1 - F^*_{|z_m|}(\xi) \right]^{Q_c - 1} \left\{ e^{-\frac{(\xi-\kappa)^2}{2\alpha}} + e^{-\frac{(\xi+\kappa)^2}{2\alpha}} \right\} \mathrm{d}\xi, \tag{37}$$

where

$$F^*_{|z_m|}(\xi) = F_{|z_m|}\left(\xi \sqrt{\sum_{l=1}^{L} \lambda_l^2 E_s N_0} \right) = \frac{1}{2} \left[\mathrm{erf}\left(\frac{\xi - \kappa}{\sqrt{2\alpha}} \right) + \mathrm{erf}\left(\frac{\xi + \kappa}{\sqrt{2\alpha}} \right) \right]. \tag{38}$$

Considering the L independent and identically distributed (i.i.d) Rayleigh-fading channels, the probability density function of the instantaneous symbol SNR γ_s is expressed as [15], [24], [47]

$$f(\gamma_s) = \frac{\gamma_s^{L-1}}{(L-1)!\bar{\gamma}_c^{L}} \exp\left(-\frac{\gamma_s}{\bar{\gamma}_c} \right), \tag{39}$$

where $\bar{\gamma}_c$ is the average symbol SNR per channel given as

$$\bar{\gamma}_c = \frac{E_s}{N_0} \mathrm{E}\left[\lambda_j^2 \right] = \frac{E_s}{N_0} \mathrm{E}\left[\lambda_l^2 \right], j \neq l, \tag{40}$$

and $\gamma_s = \frac{E_s}{N_0} \sum_{l=1}^{L} \lambda_l^2$ with $\sum_{l=1}^{L} \mathrm{E}\left[\lambda_l^2 \right] = 1$.

Finally, substituting (22) and (37) into (14), we obtain the BER of IM-MDCSK system over multipath Rayleigh fading channel given as

$$\bar{P}_{sys} = \int_0^{\infty} P_{sys} \cdot f(\gamma_s) \mathrm{d}\gamma_s. \tag{41}$$

V. Numerical Results and Discussions

In this section, computer simulations are performed to evaluate the BER performance of IM-MDCSK system over AWGN and multipath Rayleigh fading channels. Assuming that the largest multipath time delay is extremely less than symbol duration, namely $0 < \tau_{\max} \ll \beta T_c$, where T_c is the interval of chaotic samples, thus the inter-symbol interference (ISI) can be ignored. For the sake of simplicity, three-path Rayleigh fading channel with equal average power gain $\mathrm{E}\left(\lambda_1^2\right) = \mathrm{E}\left(\lambda_2^2\right) = \mathrm{E}\left(\lambda_3^2\right) = \frac{1}{3}$ and time delay $\tau_1 = 0$, $\tau_2 = T_c$, $\tau_3 = 2T_c$ is used in simulations.

A. Performance Evaluation

Fig. 7 shows the BER performance of IM-MDCSK system over AWGN channel with $\beta = 256$, $N = 3$, $Q_c = 2$ and $M = 2, 4, 8, 16$. Clearly, there is a good match between the analytical and simulation results, which verifies our theoretical derivations. When $M = 4$, IM-MDCSK system achieves better BER performance than $M = 2$. Whereas, the BER performance of IM-MDCSK system, except the above special case, is deteriorating with the increasing M. The main reason is that the decision boundaries of M-ary constellation are decreasing when M increases. From another view, IM-MDCSK system

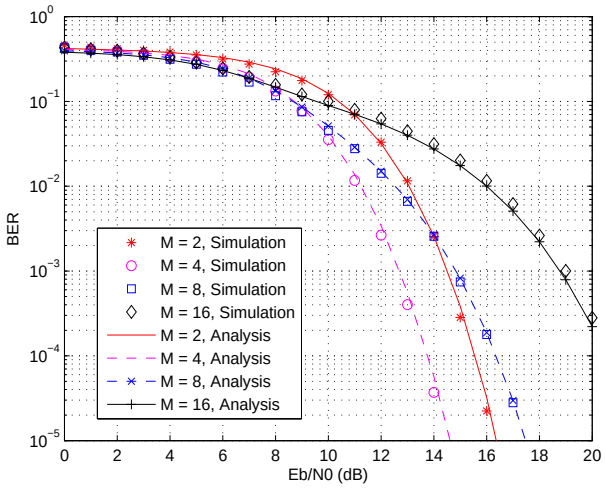

Fig. 7. The influence of M on IM-MDCSK performance for $\beta = 256$, $N = 3$, $Q_c = 2$ and $M = 2, 4, 8, 16$ over AWGN channel.

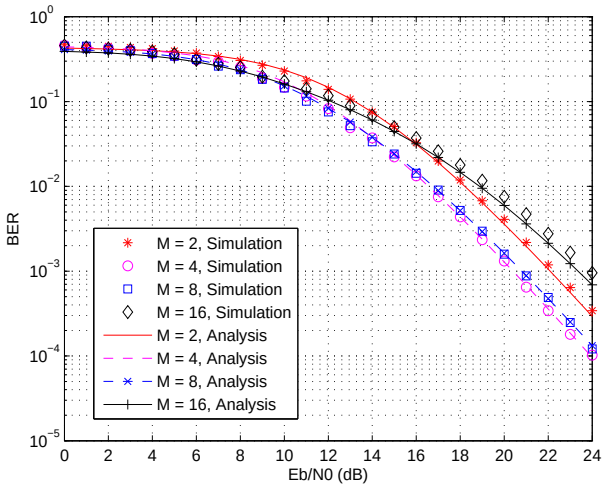

Fig. 8. The influence of M on IM-MDCSK performance for $\beta = 512$, $N = 3$, $Q_c = 2$ and $M = 2, 4, 8, 16$ over multipath Rayleigh fading channel.

can be applied to higher data rate scenarios by sacrificing a certain BER performance. In addition, the simulated and theoretical results for IM-MDCSK system over multipath Rayleigh fading channel with $\beta = 512$, $N = 3$, $Q_c = 2$ and $M = 2, 4, 8, 16$ are depicted in Fig. 8. As observed in this figure, the analytical results also match simulation results well. Unlike the case of AWGN channel, the best BER performance of IM-MDCSK system appears in medium modulation orders (i.e., $M = 4$ or 8). And the BER performance gap between $M = 2$ and $M = 16$ is less than 1dB at BER level 10^{-3}.

Fig. 9 and Fig. 10 compare the BER performance of IM-MDCSK system with different m_c over AWGN and multipath Rayleigh fading channels, respectively. As shown in Fig. 9, the BER performance of IM-MDCSK system is improved when m_c increases, and the performance gain is almost 4dB over AWGN channel between $m_c = 1$ and $m_c = 4$ at BER level 10^{-5}. In multipath Rayleigh fading channel, as observed in

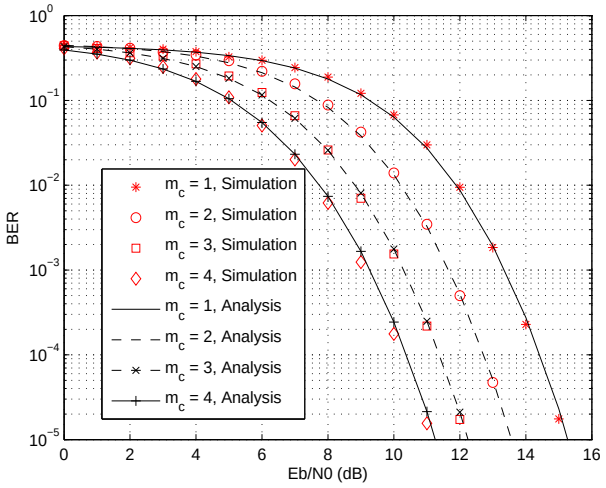

Fig. 9. The effect of m_c on IM-MDCSK performance for $\beta = 256$, $M = 4$, $Q_c = 1$ and $N = 2, 4, 8, 16$, namely $m_c = 1, 2, 3, 4$, over AWGN channel.

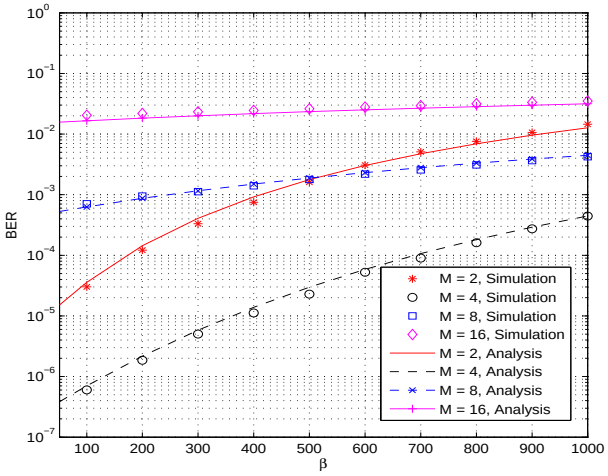

Fig. 11. The effect of β on BER performance over AWGN channel. The parameters are $\frac{E_b}{N_0} = 14$dB, $N = 4$, $Q_c = 2$ and $M = 2, 4, 8, 16$.

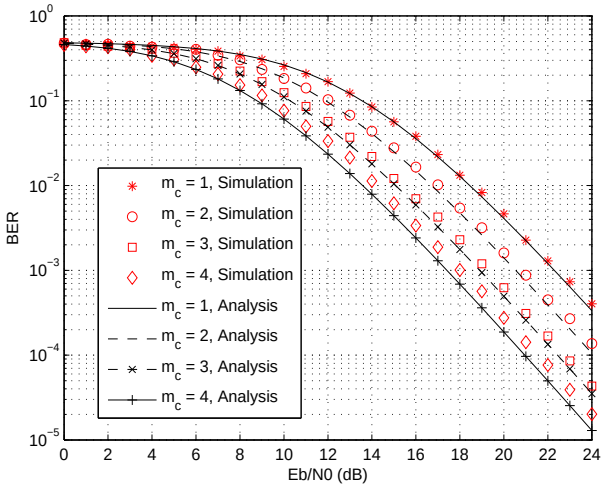

Fig. 10. The effect of m_c on IM-MDCSK performance for $\beta = 1024$, $M = 4$, $Q_c = 1$ and $N = 2, 4, 8, 16$, namely $m_c = 1, 2, 3, 4$, over multipath Rayleigh fading channel.

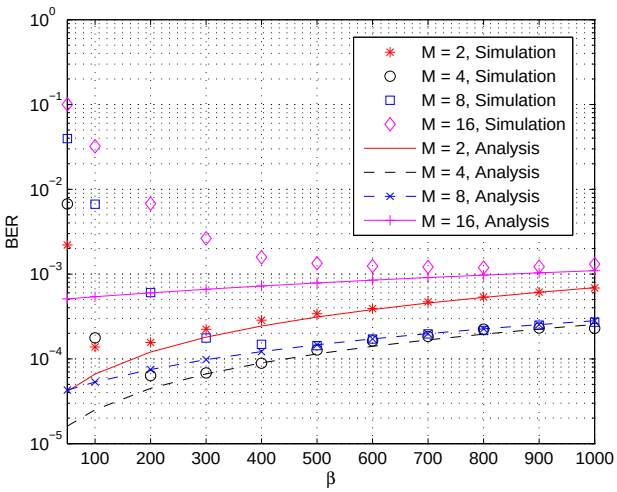

Fig. 12. The effect of β on BER performance over multipath Rayleigh fading channel. The parameters are $\frac{E_b}{N_0} = 23$dB, $N = 4$, $Q_c = 2$ and $M = 2, 4, 8, 16$.

Fig. 10, IM-MDCSK system needs more than 22dB to achieve 10^{-3} BER performance in the case of $m_c = 1$. By contrast, when $m_c = 4$, the required E_b/N_0 reduces to about 17dB. In other words, the performance improvement is approximate 5dB between $m_c = 4$ and $m_c = 1$. As a matter of fact, this phenomenon is due to that with the increasing of m_c, namely higher proportion of mapped bits corresponding to the total transmitted bits per symbol, there is more energy spending on modulated bits leading to better BER performance. Besides, analytical results match the simulated ones well, which further confirms our theoretical analysis.

The influence of β on the BER performances of IM-MDCSK system over AWGN and multipath Rayleigh fading channels are depicted in Fig. 11 and Fig. 12. In AWGN channel, the BER performance of IM-MDCSK system becomes worse when β increases. Considering a constant β, the relationship of M and its corresponding BER performance can also be observed in Fig. 11. In multipath Rayleigh fading channel, although the fitting degree is disappointed when β is small, there is a good agreement between the simulated and analytical results in the case of large β. The multipath delay is ignored in our theoretical derivations, however the assumption of $0 < \tau_{\max} \ll \beta T_c$, namely the maximum multipath delay is far less than symbol duration, is not satisfied in simulations when β is small, resulting in the mismatch between analytical and simulation results.

B. Comparisons with Other Chaotic Schemes

In order to further confirm the excellent BER performance of IM-MDCSK system, we put IM-MDCSK, M-ary DCSK and other up-to-date IM-based non-coherent chaotic communication systems into comparisons over AWGN and multipath Rayleigh fading channels. And the BER performance of DCSK

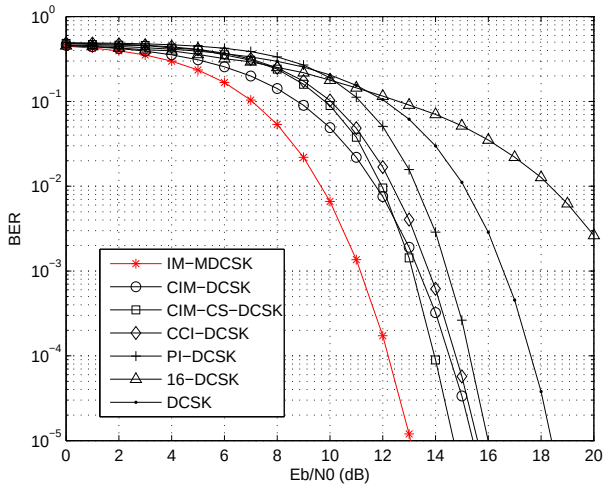

Fig. 13. BER performance comparisons of IM-MDCSK to M-ary DCSK and other up-to-date IM-based non-coherent chaotic communication systems over AWGN channel with $\beta = 256$.

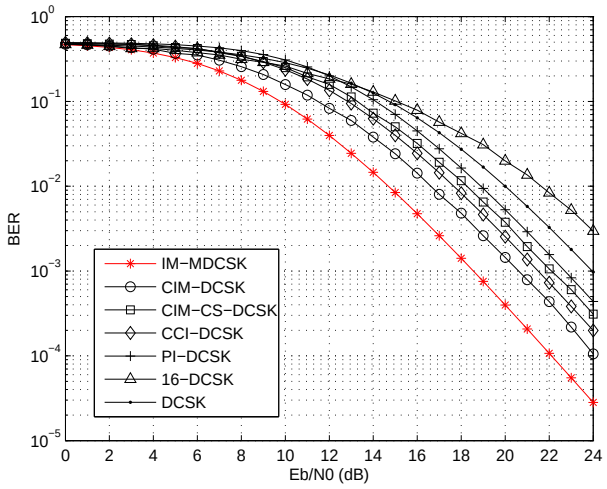

Fig. 14. BER performance comparisons of IM-MDCSK to M-ary DCSK and other up-to-date IM-based non-coherent chaotic communication systems over multipath Rayleigh fading channel with $\beta = 512$.

system is listed as well for reference. $N = 8$, $Q_c = 1$ and $n_t = 1$ are provided for IM-MDCSK system and $P = 8$ is used in CIM-DCSK simulation. As for PI-DCSK system, the main parameter is the specific modulation order M_t which is set to 16. Accordingly, the total numbers of transmitted bits per symbol in IM-MDCSK, CIM-DCSK and PI-DCSK systems are equal to 4, which includes 1 modulated bits and 3 mapped bits. Similarly, the total numbers of transmitted bits per CCI-DCSK symbol and CIM-CS-DCSK symbol are set to 4, so does 16-ary DCSK system.

As observed in Fig. 13, IM-MDCSK system outperforms 16-ary DCSK and all state-of-the-art IM-based chaotic communication systems above. For example, the performance improvement for IM-MDCSK system over other IM-based chaotic modulation system is $1.5 \sim 3$dB at BER level 10^{-5}. In Fig. 14, we compare the BER performance of IM-MDCSK and other chaotic communication systems over multipath Rayleigh fading channel. Although CIM-DCSK system achieves 3dB performance gain in BER level 10^{-3} compared to DCSK system, IM-MDCSK system performs over 5dB better than DCSK system in the same BER level above. In other words, it offers IM-MDCSK system 2dB performance gain superior to CIM-DCSK system. Therefore, the BER performance of IM-MDSK system clearly outperforms M-ary DCSK and other IM-based chaotic communication systems over both AWGN and multipath Rayleigh fading channels.

As shown in Fig. 15, the BER performance of IM-MDCSK system in comparison with CIM-DCSK, PI-DCSK and M-ary DCSK systems is evaluated over two-path Rayleigh fading channel with $\beta = 100$, the gains $\mathrm{E}\left(\lambda_1^2\right) = \frac{2}{3}$, $\mathrm{E}\left(\lambda_2^2\right) = \frac{1}{3}$ and time delay $\tau_1 = 0$, $\tau_2 = 12$. $N = 4$, $Q_c = 1$ and $n_t = 1$ are used in IM-MDCSK simulation. The total numbers of transmitted bits per symbol for IM-MDCSK, CIM-DCSK, PI-DCSK and 8-ary DCSK are the same, which are equal to 3. Since the maximum delay spread $\tau_2 = 12$ is not much less than β, the inter-symbol interference can not be ignored. Clearly,

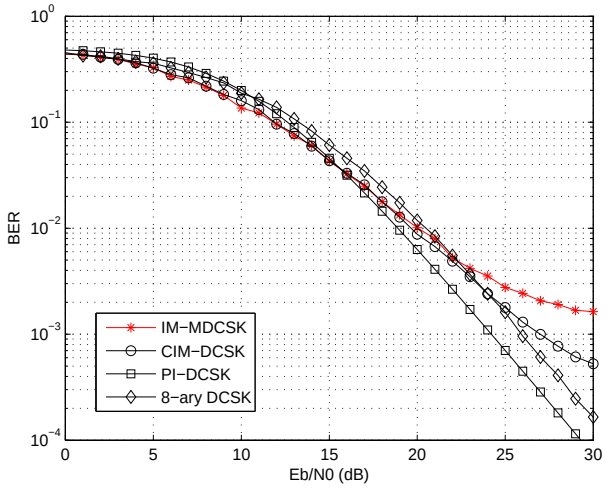

Fig. 15. BER performance comparisons of IM-MDCSK to other non-coherent chaotic communication systems over two-path Rayleigh fading channel with $\beta = 100$, the gains $\mathrm{E}\left(\lambda_1^2\right) = \frac{2}{3}$, $\mathrm{E}\left(\lambda_2^2\right) = \frac{1}{3}$ and time delay $\tau_1 = 0$, $\tau_2 = 12$.

the BER performance of IM-MDCSK system is inferior to it rivals in high E_b/N_0 range, because for larger delay spread the influence of inter-symbol interference increases significantly which results in the poor BER performance of IM-MDCSK system. In contrast, PI-DCSK system shows strong robustness when the delay spread is large. Moreover, another limitation of IM-MDCSK system is that it does not have the advantage of multiple access in comparison to PI-DCSK system.

VI. Conclusion

A new non-coherent chaotic communication scheme with index modulation named IM-MDCSK is proposed. As an M-ary constellation modulation scheme and combining with index modulation technique, IM-MDCSK system is capable of improving the data rate by adding more additional mapped bits

and adjusting M-ary constellation parameters. Furthermore, we derive the analytical BER expressions for the proposed system over additive white Gaussian noise and multipath Rayleigh fading channels, and simulation results match the analytical results well, which verifies our theoretical derivations. Although the hardware complexity of IM-MDCSK system is generally higher than CIM-DCSK, PI-DCSK and CCI-DCSK systems, the spectral efficiency of IM-MDCSK scheme with reasonable parameters is superior to its rivals. In addition, IM-MDCSK system can achieve better BER performance than M-ary DCSK and other state-of-the-art IM-based chaotic communication systems. Considering the demand of higher data rate and the rugged environment of future wireless communication, IM-MDCSK system is competitive and up-and-coming.

REFERENCES

[1] F. C. M. Lau and C. K. Tse, *Chaos-based digital communication systems: Operating principles, analysis methods, and performance evaluation*, Berlin, Germany: Springer-Verlag, 2003.

[2] L. Ye, G. Chen, and L. Wang, "Essence and advantages of FM-DCSK versus conventional spread-spectrum communication methods," *Circuits, Syst. Signal Processing*, vol. 24, pp. 657-673, Oct. 2005.

[3] J. Yu and Y. Yao, "Detection performance of chaotic spreading LPI waveforms," *IEEE Trans. Wireless Commun.*, vol. 4, no. 2, pp. 390-396, Mar. 2005.

[4] H. Dedieu and M. P. Kennedy, "Chaos shift keying: Modulation and demodulation of a chaotic carrier using self-synchronization Chua's circuit," *IEEE Trans. Circuits Syst.-II: Analog Digit. Signal Process.*, vol. 40, no. 10, pp. 634-642, Oct. 1993.

[5] G. Kolumbán, M. Kennedy, and L. Chua, "The role of synchronization in digital communications using chaos. I. Fundamentals of digital communications," *IEEE Trans. Circuits Syst. I, Fundam. Theory Appl.*, vol. 44, no. 10, pp. 927-936, Oct. 1997.

[6] G. Kolumbán, M. Kennedy, and L. Chua, "The role of synchronization in digital communications using chaos. II. Chaotic modulation and chaotic synchronization," *IEEE Trans. Circuits Syst. I, Fundam. Theory Appl.*, vol. 45, no. 11, pp. 1129-1140, Nov. 1998.

[7] G. Kolumbán, G. K. Vizvari, W. Schwarz, and A. Abel, "Differential chaos shift keying: A robust coding for chaos communication," in *Proc. Nonlinear Dyn. Electron. Syst.*, Seville, Spain, 1996, pp. 92-97.

[8] G. Kolumbán, G. Kis, M. Kennedy, and Z. Jáko, "FM-DCSK: A new and robust solution to chaos communications," in *Proc. Int. Symp. Nonlinear Theory Appl.*, 1997, pp. 117-120.

[9] G. Kaddoum, H. Tran, L. Kong and M. Atallah, "Design of simultaneous wireless information and power transfer scheme for short reference DCSK communication systems," *IEEE Trans. Commun.*, vol. 65, no. 1, pp. 431-443, Jan. 2017.

[10] F. J. Escribano, G. Kaddoum, A. Wagemakers and P. Giard, "Design of a new differential chaos-shift-keying system for continuous mobility," *IEEE Trans. Commun.*, vol. 64, no. 5, pp. 2066-2078, May 2016.

[11] G. Kaddoum and N. Tadayon, "Differential chaos shift keying: A robust modulation scheme for power-line communications," *IEEE Trans. Circuits Syst., II, Exp. Briefs*, vol. 64, no. 1, pp. 31-35, Jan. 2017.

[12] W. Xu, L. Wang, and G. Kolumbán, "A novel differential chaos shift keying modulation scheme," *Int. J. Bifurcation Chaos*, vol. 21, no. 3, pp. 799-814, 2011

[13] M. Herceg, G. Kaddoum, D. Vranje and E. Soujeri, "Permutation index DCSK modulation technique for secure multiuser high-data-rate communication systems," *IEEE Trans. Veh. Technol.*, vol. 67, no. 4, pp. 2997-3011, April 2018.

[14] Z. Galias and G. M. Maggio, "Quadrature chaos-shift keying: Theory and performance analysis," *IEEE Trans. Circuits Syst. I, Fundam. Theory Appl.*, vol. 48, no. 12, pp. 1510-1519, Dec. 2001.

[15] L. Wang, G. Cai and G. R. Chen, "Design and performance analysis of a wew multiresolution M-ary differential chaos shift keying communication system," *IEEE Trans. Wireless Commun.*, vol. 14, no. 9, pp. 5197-5208, Sept. 2015.

[16] S. Wang and X. Wang, "M-DCSK-based chaotic communications in MIMO multipath channels with no channel state information," *IEEE Trans. Circuits Syst., II, Exp. Briefs*, vol. 57, no. 12, pp. 1001-1005, Dec. 2010.

[17] G. Cai, Y. Fang, G. Han, F. C. M. Lau and L. Wang, "A square-constellation-based M-ary DCSK communication system," *IEEE Access*, vol. 4, pp. 6295-6303, 2016.

[18] G. Cai, Y. Fang, G. Han, L. Wang and G. Chen, "A new hierarchical M-ary DCSK communication system: Design and analysis," *IEEE Access*, vol. 5, pp. 17414-17424, 2017.

[19] G. Kis, "Performance analysis of chaotic communication systems," Ph.D. dissertation, Dept. Meas. Inf. Syst., Budapest Univ. Technol. Econ., Budapest, Hungary, 2005.

[20] W. Xu, L. Wang, and G. Kolumbán, "A new data rate adaption communications scheme for code-shifted differential chaos shift keying modulation," *Int. J. Bifurcation Chaos*, vol. 22, no. 8, pp. 1-8, 2012.

[21] T. Huang, L. Wang, W. Xu, and F. C. M. Lau, "Multilevel code-shifted differential-chaos-shift-keying system," *IET Commun.*, vol. 10, no. 10, pp. 1189-1195, 2016.

[22] G. Kaddoum and F. Gagnon, "Design of a high-data-rate differential chaos-shift keying system," *IEEE Trans. Circuits Syst., II, Exp. Briefs*, vol. 59, no. 7, pp. 448-452, Jul. 2012.

[23] H. Yang, W. K. Tang, G. Chen, and G.-P. Jiang, "System design and performance analysis of orthogonal multi-level differential chaos shift keying modulation scheme," *IEEE Trans. Circuits Syst. I, Reg. Papers*, vol. 63, no. 1, pp. 146-156, Jan. 2016.

[24] G. Kaddoum, F. Richardson and F. Gagnon, "Design and analysis of a multi-carrier differential chaos shift keying communication system," *IEEE Trans. Commun.*, vol. 61, no. 8, pp. 3281-3291, August 2013.

[25] M. Katoozian, K. Navaie and H. Yanikomeroglu, "Utility-based adaptive radio resource allocation in OFDM wireless networks with traffic prioritization," *IEEE Trans. Wireless Commun.*, vol. 8, no. 1, pp. 66-71, Jan. 2009.

[26] G. Kaddoum and E. Soujeri, "NR-DCSK: A noise reduction differential chaos shift keying system," *IEEE Trans. Circuits Syst., II, Exp. Briefs*, vol. 63, no. 7, pp. 648-652, July 2016.

[27] W. Xu, L. Wang and T. Huang, "Optimal power allocation in MC-DCSK communication system," in *Proc. 14th International Symposium on Communications and Information Technologies (ISCIT)*, Incheon, 2014, pp. 313-317.

[28] H. Yang, G. Jiang, W. K. S. Tang, G. Chen and Y. Lai, "Multi-carrier differential chaos shift keying system with subcarriers allocation for noise reduction," *IEEE Trans. Circuits Syst., II, Exp. Briefs*, vol. 65, no. 11, pp. 1733-1737, Nov. 2018.

[29] G. Kaddoum, "Design and performance analysis of a multiuser OFDM based differential chaos shift keying communication system," *IEEE Trans. Commun.*, vol. 64, no. 1, pp. 249-260, Jan. 2016.

[30] E. Basar, M. Wen, R. Mesleh, M. Di Renzo, Y. Xiao and H. Haas, "Index modulation techniques for next-generation wireless networks," *IEEE Access*, vol. 5, pp. 16693-16746, 2017.

[31] G. Kaddoum, M. F. A. Ahmed and Y. Nijsure, "Code index modulation: A high data rate and energy efficient communication system," *IEEE Commun. Lett.*, vol. 19, no. 2, pp. 175-178, Feb. 2015.

[32] G. Kaddoum, Y. Nijsure and H. Tran, "Generalized code index modulation technique for high-data-rate communication systems," *IEEE Trans. Veh. Technol.*, vol. 65, no. 9, pp. 7000-7009, Sept. 2016.

[33] W. Xu, T. Huang and L. Wang, "Code-shifted differential chaos shift keying with code index modulation for high data rate transmission," *IEEE Trans. Commun.*, vol. 65, no. 10, pp. 4285-4294, Oct. 2017.

[34] Y. Tan, W. Xu, T. Huang and L. Wang, "A multilevel code shifted differential chaos shift keying scheme with code index modulation," *IEEE Trans. Circuits Syst., II, Exp. Briefs*, vol. 65, no. 11, pp. 1743-1747, Nov. 2018.

[35] M. Herceg, D. Vranješ, G. Kaddoum and E. Soujeri, "Commutation code index DCSK modulation technique for high-data-rate communication systems," *IEEE Trans. Circuits Syst., II, Exp. Briefs*, vol. 65, no. 12, pp. 1954-1958, Dec. 2018.

[36] G. Kaddoum, E. Soujeri and Y. Nijsure, "Design of a short reference noncoherent chaos-based communication systems," *IEEE Trans. Commun.*, vol. 64, no. 2, pp. 680-689, Feb. 2016.

[37] W. Xu, Y. Tan, F. C. M. Lau and G. Kolumbán, "Design and optimization of differential chaos shift keying scheme with code index modulation," *IEEE Trans. Commun.*, vol. 66, no. 5, pp. 1970-1980, May 2018.

[38] G. Cheng, L. Wang, W. Xu and G. Chen, "Carrier index differential chaos shift keying modulation," *IEEE Trans. Circuits Syst., II, Exp. Briefs*, vol. 64, no. 8, pp. 907-911, Aug. 2017.

[39] G. Cheng, L. Wang, Q. Chen and G. Chen, "Design and performance analysis of generalised carrier index M-ary differential chaos shift keying modulation," *IET Commun.*, vol. 12, no. 11, pp. 1324-1331, June 2018.

[40] G. Kolumbán, Z. Jako and M. P. Kennedy, "Enhanced versions of DCSK and FM-DCSK data transmission systems," in *Proc. the 1999 IEEE International Symposium on Circuits and Systems VLSI (Cat. No.99CH36349)*, Orlando, FL, 1999, pp. 475-478, vol.4.
[41] H. Yang and G. Jiang, "High-efficiency differential-chaos-shift-keying scheme for chaos-based noncoherent communication," *IEEE Trans. Circuits Syst., II, Exp. Briefs*, vol. 59, no. 5, pp. 312-316, May 2012.
[42] H. Yang and G. Jiang, "Reference-modulated DCSK: A novel chaotic communication scheme," *IEEE Trans. Circuits Syst., II, Exp. Briefs*, vol. 60, no. 4, pp. 232-236, April 2013.
[43] E. Başar, Ü. Aygölü, E. Panayırcı and H. V. Poor, "Orthogonal frequency division multiplexing with index modulation," *IEEE Trans. Signal Process.*, vol. 61, no. 22, pp. 5536-5549, Nov.15, 2013.
[44] Y. Xia, C. Tse, and F. C. Lau, "Performance of differential chaos-shiftkeying digital communication systems over a multipath fading channel with delay spread," *IEEE Trans. Circuits Syst., II, Exp. Briefs*, vol. 51, no. 12, pp. 680-684, Dec. 2004.
[45] H. Yang, W. K. S. Tang, G. Chen and G. Jiang, "Multi-carrier chaos shift keying: System design and performance analysis," *IEEE Trans. Circuits Syst. I, Reg. Papers*, vol. 64, no. 8, pp. 2182-2194, Aug. 2017.
[46] X. Cai, W. Xu, D. Wang, S. Hong and L. Wang, "An M-ary orthogonal multilevel differential chaos shift keying system with code index modulation," *IEEE Trans. Commun.*, vol. 67, no. 7, pp. 4835-4847, July 2019.
[47] J. G. Proakis and M. Salehi, *Digital Communications*. New York, NY, USA: McGraw-Hill, 2007.

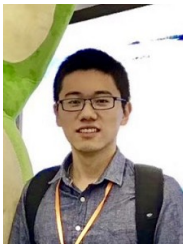

Xiangming Cai received the B.Sc. degree in information engineering from Guangdong University of Technology, Guangzhou, China, in 2017. He is currently pursuing the M.Sc. degree in the Department of Information and Communication Engineering, Xiamen University, Fujian, China. His research interests include chaos-based digital communications and their applications to wireless communications.

Weikai Xu (S'10-M'12) received the B.S. degree in electronic engineering from Three Gorges College, Chongqing, China, in 2000, the M.Sc. degree in communication and information system from the Chongqing University of Posts and Telecommunications, Chongqing, China, in 2003, and the Ph.D. degree in electronic circuit and system from the Xiamen University of China, Xiamen, China, in 2011. From 2003 to 2012, he was a Teaching Assistant, and Assistant Professor in Communication Engineering of Xiamen University. He is now an Associate Professor in Information and Communication Engineering of Xiamen University. His research interests include chaotic communications, underwater acoustic communications, channel coding, cooperative communications and ultra-wideband.

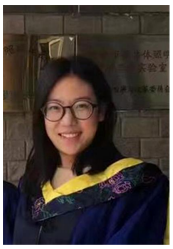

Meiyuan Miao received the B.Sc. degree in communication engineering, and the M.Sc. degree in Optics Engineering from Dalian polytechnic University, Dalian, China, in 2014 and 2017, respectively. She is currently working toward the Ph.D. degree in the Department of Information and Communication Engineering, Xiamen University, Xiamen, China. Her research interests include chaotic communications, PLC , and coded modulations.

Lin Wang (S'99-M'03-SM'09) received the M.Sc. degree in applied mathematics from the Kunming University of Technology, China, in 1988, and the Ph.D. degree in electronics engineering from the University of Electronic Science and Technology of China, China, in 2001. From 1984 to 1986, he was a Teaching Assistant with the Mathematics Department, Chongqing Normal University. From 1989 to 2002, he was a Teaching Assistant, a Lecturer, and then an Associate Professor in applied mathematics and communication engineering with the Chongqing University of Post and Telecommunication, China. From 1995 to 1996, he was with the Mathematics Department, University of New England, Armidale, NSW, Australia, for one year. In 2003, he was a Visiting Researcher with the Center for Chaos and Complexity Networks, Department of Electronic Engineering, City University of Hong Kong, for three months. In 2013, he was a Senior Visiting Researcher with the Department of ECE, University of California at Davis, Davis, CA, USA. From 2003 to 2012, he was a Full Professor and an Associate Dean with the School of Information Science and Engineering, Xiamen University, China. He has been a Distinguished Professor since 2012. He holds 14 patents in the field of physical layer in digital communications. He has authored over 100 journal and conference papers. His current research interests are in the area of channel coding, joint source and channel coding, chaos modulation, and their applications to wireless communication and storage systems.